Journal of Evolutionary Biology, 2025, **0**, 1–12
https://doi.org/10.1093/jeb/voaf112
Advance access publication 24 September 2025
Research Article

JOURNAL OF
Evolutionary Biology
eseb

Major histocompatibility complex modulation of *Batrachochytrium dendrobatidis* and *Ranavirus* infections in amphibians

Maria Cortazar-Chinarro[1,2,3], Alex Richter-Boix[4], Peter Halvarsson[5], Gemma Palomar[6], Jaime Bosch[7]

[1]MEMEG/Department of Biology, Lund University, Lund, Sweden
[2]Animal Ecology/Department of Ecology and Genetics, Uppsala University, Uppsala, Sweden
[3]Department of Earth Ocean and Atmospheric Sciences/Faculty of Science, Vancouver, Canada
[4]Center for Advanced Studies of Blanes (CEAB-CSIC), Blanes, Spain
[5]Parasitology/Department of Biomedical Sciences and Veterinary Public Health, Swedish University of Agricultural Sciences, Uppsala, Sweden
[6]Department of Genetics, Physiology and Microbiology, Faculty of Biological Sciences, Complutense University of Madrid, Madrid, Spain
[7]IMIB-Biodiversity Research Institute, Universidad de Oviedo-CSIC-Principality of Asturias, Mieres, Asturias, Spain

Handling editor: Rebekah Rogers, Associate editor: Jun Kitano

Corresponding author: Maria Cortazar-Chinarro, Animal Ecology/Department of Ecology and Genetics, Uppsala University, Norbyvagen 18D 75236 Uppsala, Sweden. Email: maria.cortazar@ebc.uu.se

Abstract

Genetic variation in immune genes is an important component of genetic diversity. The genes in the major histocompatibility complex (MHC) provide an excellent model system for studying the mechanisms that generate and maintain genetic diversity in natural populations. While both demographic factors and pathogen-mediated selection processes contribute to the extreme diversity observed in the MHC systems, determining the relative importance of these evolutionary mechanisms has remained challenging. We investigated the role of pathogen-mediated selection in driving MHC diversity in 3 amphibian species: *Ichthyosaura alpestris*, *Pleurodeles waltl*, and *Pelophilax perezi*. Our study examined the relationships between individual MHC diversity, infection status, infection intensity, and co-infection with 2 major amphibian pathogens: *Batrachochytrium dendrobatidis* (*Bd*) and *Ranavirus* sp. (*Rv*) in natural populations. Our research demonstrated significant differences in *Bd* and *Rv* infection intensities among individuals with varying numbers of MHC loci. However, co-infection showed no discernible influence on infection intensities. We observed stronger associations of specific MHC alleles and supertypes with infection intensity and status in *I. alpestris*. These findings suggest that, in the context of multi-host infections, MHC genes may provide valuable insights into the evolutionary forces shaping MHC diversity, although the specific effects of individual MHC alleles on disease dynamics are yet to be clarified.

Keywords: amphibian, co-infections dynamics, chytrid fungus, viruses, infection status

Introduction

Host–pathogen coevolution plays a significant role in maintaining genetic variation in immune genes, influencing crucial evolutionary processes including pathogen virulence evolution (McDonald et al., 2023), kin recognition (Sommer, 2005), and sexual selection (Grieves et al., 2019; van Oosterhout, 2009; Winternitz et al., 2013). The major histocompatibility complex (MHC) genes, particularly MHC class II, exemplify genetic polymorphism maintained through strong diversifying and balancing selection, thereby maintaining high diversity within natural populations (Spurgin & Richardson, 2010). However, despite their ecological and evolutionary significance, the processes driving MHC evolution remain incompletely understood (Radwan et al., 2020).

Several non-exclusive evolutionary mechanisms likely contribute to maintaining MHC diversity under pathogen-imposed selection at a population level (Jan Ejsmond et al., 2014). For example, the heterozygote advantage theory proposes that individuals that are heterozygous at MHC loci may have a selective advantage compared to homozygotes, and this advantage may help maintain allelic c diversity in a population (Doherty & Zinkernagel, 1975; Penn et al., 2002). Supporting this hypothesis, several studies have found positive linear relationships between MHC diversity and various fitness traits (Thoss et al., 2011; Whittingham et al., 2015), along with negative associations with pathogen infection prevalence or infection intensity (Radwan et al., 2012; Slade et al., 2017). However, an excess of heterozygotes can alternatively be explained by rare-allele advantage or negative frequency-dependent selection, where heterozygotes may be favoured not for their heterozygosity itself, but because they are carrying rare or novel MHC variants (i.e., resistance alleles) (Spurgin & Richardson, 2010). Recent theoretical studies suggest that frequency-dependent selection mechanisms may play a key role in helping hosts cope with infections in natural populations (Ejsmond & Radwan, 2015). Although di-

Received August 22, 2024; revised August 19, 2025; accepted September 4, 2025

rect evidence for frequency-dependent selection mechanisms primarily comes from experimental studies and long-term monitoring of MHC diversity in the wild (Migalska et al., 2022; Phillips et al., 2018), there is growing empirical support for associations between MHC variation and disease dynamics such as infection prevalence or parasite load in wildlife populations (O'Reilly et al., 2023; Osborne et al., 2017; Radwan et al., 2020; Westerdahl, 2007).

The immunogenetic optimality hypothesis presents an alternative to the heterozygote advantage theory (Nowak et al., 1992). This hypothesis suggests that while higher heterozygosity confers broader pathogen recognition, it also increases the risk of autoimmune diseases and reduces T-cell functionality at high individual MHC diversity levels (Migalska et al., 2022; Woelfing et al., 2009). According to this hypothesis, optimal infection resistance occurs at intermediate levels of individual MHC diversity (Kalbe et al., 2009; Wegner et al., 2003). Several studies have found support for the MHC optimality hypothesis across various vertebrate groups, including mammals, birds, reptiles, and fish (Bonneaud et al., 2004; Hablützel et al., 2014; Kloch et al., 2010; Madsen & Ujvari, 2006). An example comes from studies of the three-spined stickleback, where individuals with intermediate number of MHC alleles showed the lowest disease susceptibility when facing concurrent pathogen infections in wild populations (Wegner et al., 2003). However, not all studies have detected benefits of intermediate MHC diversity (Radwan et al., 2012; Sepil et al., 2013). These conflicting results raise an important question: do the advantages of intermediate diversity depend on the species studied and/or the intensity of parasitic infection (Milinski, 2006)?

Among vertebrates, amphibians have experienced unprecedented impacts from two emerging diseases: chytridiomycosis and ranavirosis (Fisher & Garner, 2020; Miller et al., 2011; Scheele et al., 2019; Skerratt et al., 2007). Chytridiomycosis, caused by the fungal pathogens *Batrachochytrium dendrobatidis* (*Bd*) and the recently discovered *Batrachochytrium salamandrivorans* (*Bsal*), has severely affected amphibian populations (Martel et al., 2014). Simultaneously, ranavirosis, caused by the viral lineage *Ranavirus* (*Rv*) within the family Iridoviridae, has further contributed to amphibian declines (Brunner et al., 2015) as reviewed by Thumsová et al. (2023). While co-infection by both pathogens has been observed frequently (Herczeg et al., 2021; Olori et al., 2018), our understanding of within-host pathogen interactions and population adaptation remains limited. Some studies suggest that antagonistic interactions between co-infecting pathogens may reduce disease severity for the host (Stutz et al., 2018; Whitfield et al., 2013). However, others either failed to confirm this interaction (Warne et al., 2016) or have found that synergistic interactions may actually increase disease severity (Bosch et al., 2020) specifically in a multi-host context. The interplay of chytridiomycosis and host immune MHC diversity has been characterized in several amphibian species to date. Most research has focused on investigating the connection between MHC class II diversity (including nucleotide and amino acid sequence polymorphism) and infection (Cortazar-Chinarro et al., 2022; Fu et al., 2023; Trujillo et al., 2021). Studies have also revealed relationships between specific MHC alleles or supertypes with infection (Belasen et al., 2022). These investigations have demonstrated positive selection acting on MHC alleles (Bataille et al., 2015; May et al., 2011; Savage & Zamudio, 2016) and heterozygosity advantage (Belasen et al., 2019; Savage & Zamudio, 2011). The exceptional polymorphism observed in amphibian MHC class II genes is believed to have evolved as a response to pathogen diversity (Savage & Zamudio, 2011; Sommer, 2005). While many studies have explored the relationship between MHC class II and *Bd*, evidence linking MHC II to *Rv* susceptibility was lacking until recently (Savage et al., 2019). However, despite the frequent occurrence of co-infections in natural populations, research on how co-infection dynamics and multi-host pathogens influence the immunological response remains limited (Hoarau et al., 2020).

In this study, we investigated evolutionary mechanisms potentially associated with the two deadliest amphibian pathogens (*Bd* and *Rv*) and their impact on MHC class II genetic diversity—a region recognized as the most polymorphic among vertebrates (Jones et al., 2006; Kaufman et al., 1985; Klein, 1979). We conducted this study across three amphibian species: *Ichthyosaura alpestris*, *Pleurodeles waltl*, and *Pelophilax perezi* investigating relationships between pathogen prevalence, infection intensities, and MHC gene diversity. We also explored associations between specific MHC alleles/supertypes and varying levels of infection across species. To study these associations, we used a supertype approach, where supertypes are defined as groups of MHC molecules with similar peptide-binding functions. This provides a robust framework for examining pathogen-mediated selection mechanisms (Spurgin & Richardson, 2010). We hypothesize that allele diversity might be reduced in infected and co-infected individuals, with different allele frequencies between infection groups, potentially diminishing their ability to cope effectively with infections. Our study emphasizes the importance of considering MHC/pathogen associations from a broader perspective in immunogenetic studies of amphibians in the wild, particularly by examining multiple pathogens simultaneously, which is a key strength of this research.

Methods

Sample collection

We sampled a total of 177 amphibians from three species: 69 Alpine newt (*Ichthyosaura alpestris*), 57 Iberian ribbed newt (*Pleurodeles waltl*), and 51 Iberian green frog (*Pelophylax perezi*). Samples were collected from two locations in the Iberian Peninsula: Picos de Europa and the Zamora province in 2020–2022 (Figure 1; see Bielby et al., 2021; Bosch et al., 2020; Thumsová et al., 2024, for a detailed description of the study areas and amphibian assemblages). These locations were selected because they have experienced significant mass mortalities and population declines in recent years due to ranavirosis and chytridiomycosis, making them ideal for studying co-infection dynamics.

Compared to other species in the Iberian Peninsula, these three species exhibited some of the highest infection prevalence when infected with a single pathogen and were among the most commonly co-infected species (*Bd* + *Rv*). Infection prevalences in *I. alpestris* ranged from 1% to 57%, depending on the pathogen and life stage. In adults, *Bd* prevalence was 7% (1% *Bd* + co-infection 6%) and *Rv* 57%. In larvae, *Bd* prevalence was 3.1% (3% *Bd* + co-infection 0.1%) and *Rv* 35% (Bielby et al., 2021; Bosch et al., 2020, 2021; Price et al., 2014). In *P. waltl*, infection rates ranged from 7% to 61% across both adults and larvae. Adults showed 77% *Bd*

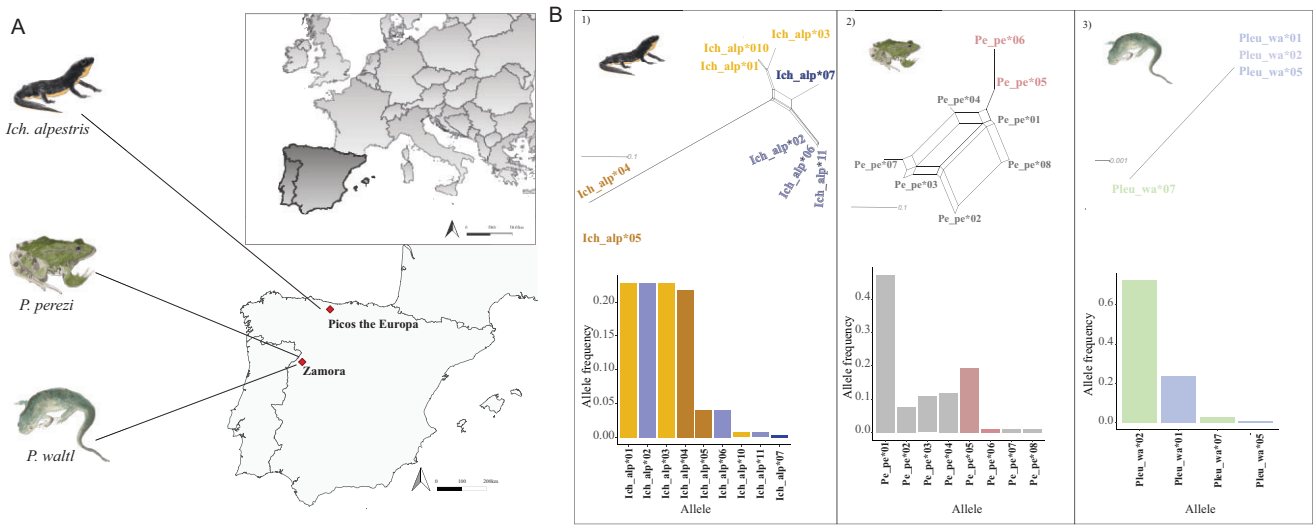

Figure 1. (A) Map showing sampling location for *I. alpestris*, *P. perezi*, and *P. waltl* in Picos the Europa and Zamora province. Amphibian illustrations were created by A. Cortazar specifically for this study. (B) Frequency distribution of major histocompatibility complex (MHC) class II exon 2 alleles based on genotyping data from 177 individuals across three species, *I. alpestris*, *P. perezi*, and *P. waltl*. Colours represent allele blocks (group of alleles that phylogenetically associated) in the three species (labelled 1, 2, and 3). An unrooted phylogenetic tree for each species illustrates the relationship between the different alleles within and between species. Alba Cortazar Chinarro is the author of the amphibian draws.

infection (61% *Bd* + 16% co-infection), 3% *Rv*, while larvae exhibited 43% *Bd* (36% *Bd* + 7% co-infection) and 14% *Rv* (Flechoso et al., 2019). For *P. perezi*, infection rates ranged from 4% to 63%. In adults, *Bd* prevalence was 69 *Bd* (63% *Bd* + co-infection 6%) and *Rv* 7%, whereas larvae had 22% *Bd* (26% *Bd* + 4% co-infection) and 20% *Rv* (Thumsová et al., 2024). Monitoring of *P. waltl* and *P. perezi* was carried out between 2018 and 2019, while *I. alpestris* was monitored initially in 2005, with continuous observation from 2007 to 2020 (Bosch et al., 2021; Flechoso et al., 2019; Thumsová et al., 2024). Mortality events were recorded in *I. alpestris* from 2005 to 2020, and in *P. waltl* and *P. perezi* in 2018 (Bosch et al., 2021; Flechoso et al., 2019; Thumsová et al., 2024). Both urodele species, *I. alpestris* and *P. waltl*, experienced recurrent mass mortalities and population declines following the emergence of *Rv*. In contrast, *P. perezi* suffered mortalities, but according to the recorded data, did not experience population declines.

Tissue samples (toe and tail clips) were collected from adult individuals for diagnostic tests. Tissue samples were collected from two locations in the Iberian Peninsula: Picos de Europa and the Zamora province in 2020–2022 (Figure 1; see Bielby et al., 2021; Bosch et al., 2020; Thumsová et al., 2024). We documented skin lesions consistent with clinical signs of ranavirosis, such as erythema or haemorrhage in infected individuals. The selected samples represented all possible infection categories: (1) *Bd* infected, (2) *Rv* infected, (3) *Bd* + *Rv* infected, and (4) non-infected (see Table S1).

DNA extraction and infection detection

Genomic DNA was extracted from the 177 individuals using the DNeasy Blood and Tissue Kit (Qiagen, Hilden, Germany). DNA concentration and purity were measured using a NanoDrop 2000 spectrophotometer and Qubit 3.0 fluorometer Quantitation Kit (Invitrogen). Two quantitave PCRs (qPCRs) were performed on a MyGo PCR machine at the IMIB-CSIC lab: one for *Bd* following Boyle et al. (2004)and one for *Rv* following Leung et al. (2017). The standard cycling conditions described by Leung et al. (2017)were used without modification: 50 °C for 2 min, 95 °C for 10 min, followed by 50 cycles of 95 °C for 15 s and 60 °C for 30 s. All samples were run in duplicate and against negative and positive controls (GeneArt Strings DNA Fragment; Life Technologies Inc., Madrid, Spain) with known concentrations of genomic equivalents (GEs). Control concentrations ranged from 0.1 to 1,000 zoospores for *Bd* and from 3 to 30,000,000 virions for *Rv* in $\log_{10}$ increments. Samples showing inhibition (non-sigmoidal amplification) were diluted to 1:100 (*Bd*) or 1:10 (*Rv*) and re-analysed. A sample was considered positive if both replicates showed infection loads > 0.1 (*Bd*) or > 3 (*Rv*) with sigmoidal amplification curves. Samples with non-sigmoidal curves or discordant replicates were re-run in duplicates, and were considered positive if both replicates were positive. Raw infection loads were calculated using the machine software based on reference standards of the known concentration of zoospore or virion. Final pathogen load was determined by averaging the two replicates from each individual.

MHC II gene 2nd exon

Single-locus amplification and preparation for sequencing

Different MHC class II exon 2 primers were used for each species. For the *I. alpestris* and *P. waltl*, primers TrMHCII1F (5′-TCTCTCCGCAGTGGACTTCGTG-3′) and TrMHCII5R (5′- CTCACGCYTCCGSTGCTCCATG -3′) from Babik et al. (2008) were used. These amplified partial fragments of the second exon (β-1 domain), 239 bp in *I. alpestris* and 355 bp in *P. waltl*. For *P. waltl* only the initial 190 bp were retained for valid allele assignment and MHC supertyping analyses due to the low quality of the reverse read and insufficient forward–reverse read overlap. For *P. perezi*, a 252-bp fragment was amplified using ForN (5′-

CCGCAGATGATTTC-3′) from Mulder et al. (2017) and RevM (5′-TCCGGTACTCACATTTCAGGTCT-3′; K. P. Mulder pers. comm.). RevM is a modified version of RevA (Mulder et al., 2017), designed to amplify a single MHC locus in ranid species, specifically *R. arvalis*. All primer combinations were validated Sanger sequencing at Macrogen, Netherlands. PCR conditions are detailed in Appendix 1. The MHC class II exon 2 amplicon sequencing library was constructed using a fusion primer approach (Cortázar-Chinarro et al., 2017). This method used primers tagged with 8-bp sequences, enabling read assignment to individuals through unique dual barcode combinations. The final pool of 12 prepools was sequenced at SNP&SEQ Technology Platform Sequencing (SciLife lab, Uppsala) using two Miseq Illumina platform runs (PE250). Detailed library construction protocol is available in Appendix 1.

Miseq data analyses

Raw sequencing data were processed by combining forward and reverse reads into a single/forward/reads using FLASH (Magoč & Salzberg, 2011) with each of the 12 amplicon pools analysed separately. The resulting 12 fastq files were converted to fasta format using Avalanche NextGen package (DNA Baser Sequence Assembler v4, 2013, Heracle BioSoft). AmpliSAS software (Sebastian et al., 2016) was used for demultiplexing, clustering, and filtering data to either *I. alpestris* or *P. perezi*. For *P. waltl*, DADA2 (Callahan et al., 2016) performed these functions. To recover reads that failed minimal overlap criteria, we used "justConcatenated=TRUE" and "verbose=TRUE" options for rescuing good-quality reads that differed in length. To ensure high replication of complex reads, samples were run in duplicates or triplicates, and samples with <300 reads were discarded for quality reasons.

The Degree of Change (DOC) method implemented in AmpliSAS was used to identify and estimate alleles (Ai) per individual without assuming specific loci numbers ((Lighten et al., 2014). This procedure identifies true alleles by detecting breakpoints in sequencing coverage between alleles within each individual, thereby avoiding the need for a manual and subjective threshold to distinguish true alleles from artefacts. After sorting alleles by coverage, the DOC statistic calculates coverage breakpoint around each allele, with the highest DOC values indicating the last true allele (Lighten et al., 2014). As we anticipated a multi-locus system, we established an additional cutoff point to simplify the genotyping process (i.e., cases with more than two alleles per sample). Following the methodology of Cortazar-Chinarro et al. (2022), we excluded alleles with less than one-third the abundance of the preceding allele within a sample. Valid alleles were imported to MEGAX (Kumar et al., 2018) for alignment and amino acid translation. Sequences containing stop codons were discarded. To verify allele authenticity, sequences were compared with existing MHC class II exon 2 sequences from related species: smooth newt (*Lissotriton montandoni*; GenBank: JN565330.1), northern crested newt (*Triturus cristatus*; GenBank: FJ448027.1), tiger salamander (*Ambystoma tigrinum*; GenBank: DQ071906.1), and moor frog (*Rana arvalis*; Cortázar-Chinarro et al., 2017). MHC exon 2 alleles were named following a modified Klein, (1975)nomenclature, species abbreviation, gene, and allele number (e.g., Ich_alp_*01).

Data analyses

MHC II exon 2 diversity

MHC class II exon 2 allele frequencies were calculated for each species and infection group (*Bd* infected, *Rv* infected, *Bd* + *Rv* infected, and non-infected; Figures S1 and S2) using ARLEQUIN v. 3.5 (Excoffier & Lischer, 2010). Differences in allele frequencies between infection groups at each location were tested using the exact test of sample differentiation based on haplotype frequencies in ARLEQUIN v. 3.5 (Excoffier & Lischer, 2010). Allele frequency plots were generated using the "ggplot2" package (Wickham, 2011) in R v. 4.1.3 (R Core Team, 2021) and SplitTree4 (Huson & Bryant, 2006).

Genetic diversity measures for the MHC II exon 2 (gene diversity [D], nucleotide diversity [π], number of pairwise nucleotide difference [k], and the average number of pairwise nucleotide differences [Δk]) were calculated for each infection group ARLEQUIN (Table S3). The average number of pairwise nucleotide differences (Δk) was calculated by dividing the sum of all k by the number of infection groups (Table S3). Loci numbers were estimated by dividing the maximum number of putatively functional MHC alleles per individual by two, assuming heterozygosity at each locus (Minias et al., 2022). Gene diversity estimations are approximate due to the multi-locus system, as in this study. Phylogenetic relationships among alleles from each amphibian species were visualized using two methods: unrooted phylogenetic network in SplitTree4 using the neighbour net method (Allman et al., 2017) (Figures S3 and S4) and a maximum likelihood phylogenetic tree with 1,000 bootstrap replicates in MEGA7 (Minias et al., 2022). A *Rana arvalis* sequence was included as an outgroup (Cortázar-Chinarro et al., 2017).

MHC II exon 2 supertyping

MHC alleles were collapsed into functional supertypes by extracting the amino acid positions of the peptide binding region (PBR) based on the human leucocyte antigen (HLA; MHC) in MHC II exon, following Meyer-Lucht and Sommer (2009) and Papadopoulos et al. (2008) (Figure S5 and Table S4). The PBR sites were characterized using five physio-chemical descriptor variables: hydrophobicity (z1), steric bulk (z2), polarity (z3), and electronic effects (z4, z5). A hierarchical clustering tree for the MHC class II exon 2 was constructed using these z-descriptors with the function *hclust* in R v. 4.1.3 (R Core Team, 2021). The optimal number of clusters was chosen based on divergence between the branches in the phylogenetic tree, with alleles within clusters were collapsed into single supertypes (Meyer-Lucht & Sommer, 2009) (Figure 2A).

We introduced "supertype$_{Genotype}$" to categorize the alleles into supertype groups for the three amphibian species. As an example, *I. alpestris*, the only species showing supertype variation, four digits represent possible supertypes (S1, S3, S5, and S6). For example, Ich_alp* 2_1_0_0 indicates two S1 alleles, one S3 allele, and no S5 or S6 alleles (Figure S6). A capital letter suffix is used to distinguish specific supertype genotypes identified within the *I. alpestris* population (e.g., Ich_alp*2_1_0_0*P, A, D, C, B, E, G). This nomenclature does not distinguish between homozygous and heterozygous alleles within supertypes. Supertype allele frequencies were plotted in Excel. MHC supertype$_{Genotype}$ frequencies for *I. alpestris* were visualized using ggplot2 (Wickham, 2011) (Figure S6).

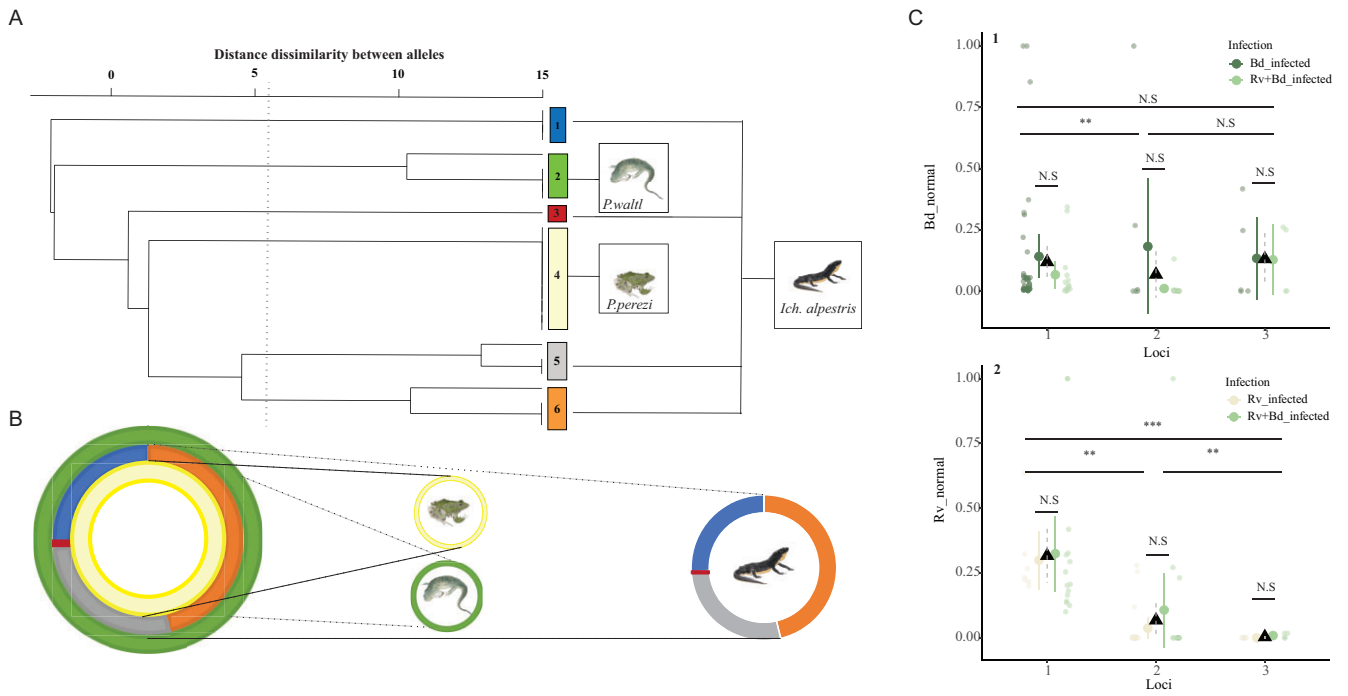

Figure 2. (A) Phylogenetic dendogram reconstruction showing functional major histocompatibility complex (MHC) class II exon 2 supertypes, represented by coloured squares. The grey line indicates the established threshold line for clustering MHC class II amino acid sequences into functional supertypes. (B) Pie charts showing supertype frequency distribution in *I. alpestris*, *P. perezi*, and *P. waltl*. Amphibian illustrations were created by A. Cortazar for this study. (C) Normalized infection loads (genome equivalents, "GE") for (1) *Batrachochytrium dendrobatidis* (*Bd*) and (2) *Ranavirus* (*Rv*) infection. Both are shown in relation to the number of MHC class II exon 2 loci (maximum of three), considering single infections (*Bd* or *Rv*) and co-infection (*Rv* + *Bd*). Black triangles indicate the average infection load per number of loci, with grey dashed lines representing standard error. Significant results from post hoc analyses are marked with asterisks (**p*-value between 0.05 and 0.01, ***p*-value between 0.01 and 0.0001, and ****p*-value <0.0001).Alba Cortazar Chinarro is the author of the amphibian draws.

MHC II exon 2 and infection

Initial infection patterns by species and location were visualized using ggplot2 (Wickham, 2011; Figure S7; A1-2, B2-2). Infection load data were normalized (0–1 scale) to enable *Bd* and *Rv* infection comparison (Table S1). Species infection patterns were analysed using generalized linear mixed models (GLMMs). For infection impact, normalized *Bd* or *Rv* load was the response variable (single infections or co-infections), with species and infection group as fixed effects. We additionally included an observation-level random effect to model overdispersion (Harrison, 2014).

To assess associations between infection load and MHC II exon 2 loci numbers, another GLMM used normalized infection load (*Bd*, *Rv*) as a response variable, with loci number and infection group as fixed effects (Figure 2C; Tables S3 and S7 and Figure S8). We used normalized *Bd* load/*Rv* load as the response variable with the number of loci and infection group as independent fixed effects. "Species" was included as a random factor due to varying MHC loci numbers in the different species. For *Rv* load, the best model included an independent dispersion parameter (=*dispformula*) for each number of loci.

All GLMMs used a zero-inflated gamma method with a "logit" link (Tables S5–S8), reflecting a data distribution and high numbers of uninfected individuals. Models were run using glmmTMB in R (Magnusson et al., 2017) and evaluated the best model based for overdispersion, homogeneity of variance, and residual normality using the Dharma package (Hartig & Hartig, 2017). Model parameters were processed using Wald tests (parameters package). Species and loci number comparisons used Turkey-adjusted post hoc tests via the emmeans R package (Lenth et al., 2019). All analyses were performed in R v. 4.1.3 (R Core Team, 2021).

The effect of MHC alleles on infection

Species-specific General Linear Models (GLMs) investigated relationships between individual MHC allele configurations and infection status (1: infected, 0: not-infected). *Pleurodeles waltl* was excluded from the analyses due to low allele numbers, as it can generate false-positive/negative relationships between infection status and alleles. The first model used infection status as response variables and specific alleles (e.g., Ich_alp *10 + Ich_alp *06 + Ich_alp *11 + Ich_alp *07 + Ich_alp *04 + Ich_alp *05) as independent variables. Second, two models used either *Bd* infection status or *Rv* infection status as response variables, and the specific alleles as independent variables. In the models, co-infected individuals were assigned to both *Bd* and *Rv* infection, respectively. Binomial error distribution with logit link function was used to assess allele-specific infection and co-infection relationships, respectively. Effects of infection on specific alleles were visualized using packages dotwhisker (Solt & Hu, 2015) and broom (Robinson, 2014) in R (Figure S9).

The effect of MHC supertypes on infection

Associations between specific MHC supertypes and infection status for *I. alpestris*, *P. perezi*, and *P. waltl* were analysed using GLMM with the glmmTMB package (Magnusson et al., 2017). Infection status was used as a response variable,

supertypes as an independent variable, and species as a random factor. Additional analyses focused on *I. alpestris* due to significant supertype–infection relationships. GLMs were used to explore specific $supertype_{Genotype}$–infection status relationships for this species. Packages dotwhisker (Solt & Hu, 2015) and broom (Robinson, 2014) were used to visualize regression coefficients showing the main effect of carrying a specific supertype and $supertype_{Genotype}$ for infection status (Figure S10). Visualizations of $supertype_{Genotype}$ and infection groups were generated using ggplot2 (Wickham, 2011) (Figure S11).

Results

Miseq run summary

The two separate sequencing runs yielded 5,675,898 reads ± 1,107,689 (*SD*) with intact primer barcode information (run 1 = 2,100,296; run 2 = 3,575,602; Table S2). The average number of reads per individual varied among species: For *P. waltl*, 2,592 ± 118 (*SD*), for *P. perezi*, 29,003 ± 341 (*SD*), and for *I. alpestris*, 23,337 ± 328 (*SD*). For MHC class II exon 2, we sequenced amplicons from 177 individuals (*I. alpestris*: $N = 69$, *P. waltl*: $N = 57$, and *P. perezi*: $N = 51$). We included a total of 129 duplicated samples (*I. alpestris*: $N = 21$, *P. waltl*: $N = 57$, and *P. perezi*: $N = 51$; Table S2). Replication rates for each Miseq run are detailed in Table S2. We discarded amplicons with <300 reads and replicates that failed to produce consistent alleles across samples. The variation in duplication numbers correlated with primer success. MHC class II exon 2 length, determined using the DOC method (Lighten et al., 2014), varied between species: *I. alpestri* (239 bp), *P. waltl* (190 bp), and *P. perezi* (252 bp).

MHC class II exon 2 diversity

We identified 21 unique MHC class II exon 2 alleles among the three species (*I. alpestris*: $N = 9$, *P. waltl*: $N = 4$, and *P. perezi*: $N = 8$; Figures S4 and S5). Four MHC class II alleles occurred at high frequency in *I. alpestris* (Ich_alp*01,02,03,04; Figure 1B), while single alleles dominated in both *P. waltl* (Pleu_wa*02) and *P. perezi* (Pe_pe*01) (Figure 1B). The exact test of sample differentiation showed no significant differences in allele frequencies among the infection groups (*Bd* infected, *Rv* infected, *Bd* + *Rv* co-infected, and non-infected), with a non-differentiation exact *p*-value of 0.99984 ± 0.00009 (based on 100,000 Markov chain iterations). MHC class II exon 2 gene diversity was lowest in *P. waltl* (0.35–0.44), compared to *P. perezi* (0.68–0.80) and *I. alpestris* (0.79–0.82) (Table S3). *Pelophilax perezi* showed lower MHC class II exon 2 nucleotide diversity (π) ($\Delta\pi$ = 0.006), but higher nucleotide differences ($\Delta k = 2.09$) compared to *P. waltl* ($\Delta\pi = 0.125$, $\Delta k = 0.66$) and *I. alpestris* ($\Delta\pi = 0.30$, $\Delta k = 1.80$) (Table S3). We identified unique alleles present across infection groups in all three species: Ich_alp*07 (*I. alpestris*; not infected group), Pe_pe*07,08 (*P. perezi*; *Bd*-infected group), and Pleu_wa*05 (*P. waltl*; *Bd*-infected group) (Figure S1; Figure 2). The remaining alleles shown in Figure S1 were shared among individuals across all infection groups. The number of valid MHC class II exon 2 alleles per individual varied by species: 1–2 alleles in *P. waltl* (average 1), 2–6 alleles in *I. alpestris* (average 2.72 ± 0.46 [*SD*]), and 1–4 alleles in in *P. perezi* (average 1.23 ± 0.42 [*SD*]). These results indicate multiple copies in the sequenced MHC class II exon 2 locus in *I. alpestris* and *P. perezi*, at least 3 and 2, respectively. Note that the results for *P. waltl* should be interpreted with caution due to the low quality of the reverse reads and insufficient overlap between forward and reverse reads, which may reduce the robustness of our findings.

Supertype and $supertype_{Genotype}$ diversity

We classified the alleles into six functional supertypes based on physio-chemical binding properties (Figure 2A; see Savage & Zamudio, 2016). After supertype assignment, all alleles clustered by species into specific supertypes. In *I. alpestris*, the supertypes showed broad distribution across the phylogeny, with distinct functionalities among different supertypes. The MHC supertype assignments were assigned to *P. waltl*: S2, *P. perezi*: S4, and *I. alpestris*: S1, S3, S5, and S6 (Figure 2A). In *I. alpestris*, we identified seven MHC $supertype_{Genotype}$, with one occurring at high frequency (Ich_alp*2_1_0_0; >50%, see Figure S6).

MHC copy number variation and infection load among study species

Bd/Rv infection load and species

The *Bd* infection load showed significant differences between species and infection groups (single-infected versus co-infected individuals) (Table S5 and Figure S8). The average infection loads (measured in genomic equivalents, GEs) along with their respective standard deviations were as follows: *P. perezi*—*Bd*: 20.11 ± 63.25 GEs; *Rv*: 5.10 ± 6.36 GEs; *P. waltl*—*Bd*: 11.94 ± 17.73 GEs; *Rv*: 5.16 ± 6.36 GEs; and *I. alpestris*—*Bd*: 1,092.96 ± 1,806.84 GEs; *Rv*: 692641.8 ± 2,554,501 GEs. This difference was most pronounced in *P. waltl* between individuals with a single *Bd* infection and those co-infected with *Rv* + *Bd*. For *Rv* infection load, we found significant differences between *I. alpestris* and *P. perezi*, but not between infection groups (Table S6). While *Ranavirus* infection was present in *I. alpestris*, its intensity was lower compared to *P. perezi* and *P. waltl*.

Bd/Rv infection load and number of loci

We observed significant differences in *Bd/Rv* infection load based on the number of alleles carried by individuals, *Bd*: $\chi^2 = 13.25$, $df = 2$, $p = 0.0013$; *Rv*: $\chi^2 = 32.81$, $df = 2$, $p < 0.001$. For *Bd* infection, individuals with one MHC class II exon 2 locus (single gene copy) had higher infection rates compared to those with two MHC loci (multiple gene copies). No significant difference was found between individuals with one versus three MHC loci. For *Rv* infection, a different pattern was found. Individuals with more MHC loci (multiple gene copies) showed lower infection rates than those with fewer loci. Notably, post hoc analyses revealed significant differences in infection load between individuals carrying one, two, and three MHC loci (Figure 2C; Tables S6 and S7). We found no significant differences between infection groups: *Bd* and *Bd* + *Rv*: $\chi^2 = 2.51$, $df = 1$, $p = 0.112$; *Rv* and *Rv* + *Bd*: $\chi^2 = 0.17$, $df = 1$, $p = 0.68$ (Figure 2C; Tables S7.B and S8.B).

The effect of specific MHC class II exon 2 configuration on infection

Allele-specific effects

Individuals of *I. alpestris* infected with *Rv* had a high probability of *Rv* infection if they carried the allele Ich_alp*04 ($\chi^2 =$ 5.94, $df = 1$, $p = 0.02$) or had a co-infection with [*Bd*] ($\chi^2 =$

8.76, $df = 1, p < 0.01$) based on a GLM analysis with binomial error distribution (Figure S9). Additionally, we found a positive association between Ich_alp*04 MHC allele and all infection types (*Bd*, *Rv*, and co-infection; see coefficient regression plot, Figure S9). In contrast, we did not find any association between Pe_pe* alleles and any infection type or co-infection in *P. perezi*. The relationship between alleles in *P. waltl* was not performed.

Supertype analysis

GLM analyses revealed a significant association between infection status and the S1 supertype, which is unique to *I. alpestris* ($\chi^2 = 4.0856$, $df = 1, p = 0.043$; Table S9). Notably, the S1 supertype includes the Ich_alp*04 allele, suggesting that the S1's significance may be linked to the Ich_alp*04 effect on infection.

Supertype$_{Genotype}$ patterns

While no statistical association was found between supertype$_{Genotype}$ and infection, descriptive analyses revealed that two *I. alpestris* individuals carrying Supertype$_{Genotype}$ Ich_alp*2_1_0_0*P and Ich_alp*2_1_1_1*C showed no infection (Figure S10). Also, the Ich_alp*2_2_0_2*E supertype$_{Genotype}$ was exclusively found in infected individuals (Figure S10).

Discussion

Our study is the first to examine MHC class II diversity in three amphibian species within a co-infection scenario. While most previous research on MHC–pathogen interactions in amphibians has focused on single-pathogen systems, our work expands this perspective by exploring host genetic responses under multi-pathogen pressure. Our findings reveal associations between specific pathogens and particular MHC alleles. Notably, individuals infected with *Bd* exhibited lower infection loads when carrying two copies of MHC genes (as further discussed in Appendix 2), which may support the immunogenetic optimality hypothesis. Our results also indicate that having more MHC copies reduced *Rv* infection load. In *I. alpestris*, we identify a significant positive association between the MHC allele Ich_alp*04 and supertype S1 with infection status for *Ranavirus* and co-infection. The presence of the specific allele (Ich_alp*04) suggests that it may confer an advantage to individuals carrying it. Such association may indicate the involvement of evolutionary host–pathogen mechanisms, including rare-allele advantage, positive selection, and/or fluctuating selection in this species (Spurgin & Richardson, 2010). However, future monitoring these allele frequencies in the population would provide empirical evidence for the selective mechanisms acting on MHC class II.

The study revealed that many individuals of *P. perezi* and *I. alpestris* carried multiple copies of MHC class II exon 2 loci, indicating single or multiple gene duplication events throughout the evolutionary history of these amphibian species. Traditionally, the MHC copy number in non-model species is estimated by screening MHC variation at the intraspecific level. This is done by detecting the maximum number of putatively functional MHC alleles in each individual and dividing it by two, assuming heterozygosity at each locus (Minias et al., 2022). Working with MHC loci that vary in number and are sometimes unknown for each individual or species presents analytical challenges and limitations. Our results provide minimum estimates of loci per individual based on the number of detected alleles, acknowledging potential limitations that it is possible that the primers did not amplify all alleles, and that homozygous loci cannot be detected using this method. These limitations could lead to overestimates of nucleotide diversity and the average number of loci per individual.

We found that the number of MHC loci and thereby alleles that an individual carries significantly correlates with infection intensity, thought is not linear. Previous research has provided evidence that individuals exhibiting increased MHC allelic diversity and higher levels of heterozygosity tend to experience reduced parasite burdens, consistent with the heterozygote advantage hypothesis (Meyer-Lucht & Sommer, 2009). Notably, individuals carrying a single MHC locus exhibited higher *Rv* infection intensity compared to those with three or more loci. This pattern suggests that an increased number of unique alleles are associated with reduced *Rv* infection loads, indicating that greater allelic diversity may confer a selective advantage within this system. These findings support the hypothesis that enhanced diversity in immune-related genes contributes to improved resistance against infections. While we cannot confirm heterozygote advantage in this specific context, our findings indicate that lower MHC copy number may negatively influence host survival. Nonetheless, experimental infection studies are needed to rigorously test and validate this hypothesis.

We also observed that individuals with an intermediated number of MHC loci had a lower infection intensity when infected with *Bd* (see Figure 2C and Table S7). This pattern was particularly evident when compared to those individuals carrying either a single MHC locus and two MHC loci, based on the analysis of average *Bd* load. Notably, for single infections, the *Bd* load appears to increase between individuals with one and those with two loci, although this difference is not statistically significant. We also found a significant relationship between the number of MHC loci and infection load in individuals infected with *Rv*. Although our analysis did not reveal any significant difference between having two or three MHC copies and *Bd* infection, these general patterns may be consistent with the immunogenetic optimality hypothesis, which suggests that individuals with an optimal level of heterozygosity gain the greatest fitness benefits (Nowak et al., 1992). Similar patterns have been demonstrated in multiple studies (Kloch et al., 2010; Madsen & Ujvari, 2006; Wegner et al., 2003, 2008). However, it is important to note that the relationship between lower infection load and an intermediate MHC allele number is not universally supported by our data. Some studies have found no such connection (Garamszegi et al., 2015; Radwan et al., 2012; Stervander et al., 2020), while others suggest that the relationship may be context-dependent (Råberg et al., 2022). Our results suggest that *Bd* infection may select for MHC and intermediate number of alleles, though further experimental validation is needed to confirm these findings.

Interestingly, we did not observe differences between *Rv*-infected and co-infected individuals, as they responded similarly across different numbers of loci. This lack of associations between infection load in co-infected individuals may indicate that the presence of *Bd* is not having an impact on *Rv* load in this species. If such an interaction existed, one might expect a scenario in which MHC alleles that confer resistance to one pathogen could increase susceptibility to another (Penn & Potts, 1999). Specifically, reciprocal patterns such as reduc-

tions in *Bd* load accompanied by increases in *Rv* load, or vice versa, associated with particular MHC alleles might be anticipated; however, these patterns were not supported by our data. The lack of a statistically significant association between the number of MHC loci and co-infection load of *Bd* and *Rv* may be attributed to multiple factors, such as climate or the pathogens' evolutionary history within the Iberian Peninsula. Amphibian population declines attributable to *Bd* were first reported in the late 1990s (Bosch & Martínez-Solano, 2003, 2006; Bosch et al., 2001), whereas mass mortalities linked to *Rv* were documented earlier, in 1988 (Price et al., 2014; Thumsová et al., 2022). Despite their long coexistence, *Bd* and *Rv* may trigger different immune responses. Specifically, the intracellular nature of *Rv* might lead to more pronounced evolution in MHC I in the host (Fu & Waldman, 2017; Warne et al., 2016), reflecting pathogen-specific adaptations across different habitats. Furthermore, amphibian susceptibility to multi-host pathogens may be modulated by ecological factors such as larval duration in aquatic environments, which has been correlated with variation in *Bd* infection intensity (Hoverman et al., 2012; Palomar et al., 2016). Collectively, these factors suggest that the complexity of host–pathogen–environment interactions limits straightforward associations between MHC diversity and infection loads in co-infected individuals, underscoring the necessity of integrating ecological and evolutionary perspectives when investigating immune gene variation.

While previous studies have investigated associations between specific MHC alleles or supertypes and pathogens in amphibians (Bataille et al., 2015; Cortazar-Chinarro et al., 2022; Savage & Zamudio, 2011), the nature of these associations and their potential contribution to amphibian anti-viral/fungal immunity remain poorly understood. This knowledge gap exists largely due to the limited number of experimental infection studies examining immune responses across amphibian species (see Bataille et al., 2015; Cortazar-Chinarro et al., 2022, for examples). Nevertheless, several RNAseq expression studies have provided valuable insights into immune responses to *Bd* in experimental settings (Chondrelli et al., 2024; Eskew et al., 2018; Savage et al., 2020). To advance our understanding, it would be valuable to investigate whether variation in functional immunity correlates with *Bd*/*Rv* infection load and prevalence within a co-infection scenario across different anuran taxa, both within and between species. This approach would enable exploration of the potential role of specific functionally expressed MHC genotypes in infection outcomes (Savage et al., 2019). We propose implementing multi-level studies encompassing: (1) immune gene diversity, (2) functional diversity, and (3) experimental infection studies conducted in controlled experiments with single and co-infected scenarios, to examine the associations between specific MHC allele configurations and outcomes such as mortality, survival, and individual fitness. By manipulating MHC genotypes and monitoring infection dynamics, we can gain insights into the direct effects of specific MHC alleles on disease susceptibility and resistance.

Our study represents the first investigation of MHC/pathogen associations within a multiple pathogen scenario, expanding the perspectives in immunogenetics studies of amphibian populations. We identified a significant association between the number of MHC class II exon 2 loci and infection intensity, consistent with the immunogenetic optimality hypothesis in the context of *Bd* infection. Furthermore, we observed that an increased number of unique MHC alleles correlated with decreased *Rv* infection loads, highlighting distinct immunogenetic dynamics for each pathogen. The development and implementation of next-generation sequencing (NGS)-based genotyping methods are essential for investigating evolutionary mechanisms that shape MHC genetic variation within and between populations, in both single and co-infected individuals. These methods will enhance our understanding of the evolutionary mechanisms governing immune genes in the hosts within a multi-infection context, helping to address this knowledge gap in a wide range of non-model organisms, particularly amphibian species.

Supplementary material

Supplementary material is available at *Journal of Evolutionary Biology* online.

Data availability

All data have been made available in Figshare: https://doi.org/10.6084/m9.figshare.c.8049589.v1

Author contributions

Maria Cortazar-Chinarro (Conceptualization, Data curation, Formal analysis, Funding acquisition, Investigation, Methodology, Project administration, Resources, Software, Supervision, Validation, Visualization, Writing – original draft, Writing – review & editing), Alex Richter-Boix (Conceptualization, Formal analysis, Investigation, Software, Writing – original draft, Writing – review & editing), Peter Halvarsson (Methodology, Software, Validation, Writing – review & editing), Gemma Palomar (Methodology, Software, Validation, Writing—review & editing), and Jaime Bosch (Conceptualization, Data curation, Funding acquisition, Writing – review & editing)

Funding

This study was supported by the Swedish Research Council (M.C.-C., international mobility grant: 2019-06352) and Organismo Autónomo Parques Nacionales of Spain (project 2399/2017; PI: J.B.).

Acknowledgments

The authors would like to acknowledge Alba Cortazar Chinarro for the amphibian water paint illustrations present in the manuscript. Camino Monsalve, Cristina Sausor, Gonzalo Alarcos, and Barbora Thumsová helped in the field and/or in the lab. We thank Helena Westerdahl for the invaluable help and support.

Conflicts of interest

All authors declare no conflict of interest.

References

Allman, E. S., Kubatko, L. S., & Rhodes, J. A. (2017). Split scores: A tool to quantify phylogenetic signal in genome-scale data. *Systematic Biology*, 66, 620–636.

Babik, W., Pabijan, M., & Radwan, J. (2008). Contrasting patterns of variation in MHC loci in the Alpine newt. *Molecular Ecology*, *17*, 2339–2355. https://doi.org/10.1111/j.1365-294X.2008.03757.x

Bataille, A., Cashins, S. D., Grogan, L., … Harlow, P. S. (2015). Susceptibility of amphibians to chytridiomycosis is associated with MHC class II conformation. *Proceedings of the Royal Society B: Biological Sciences*, *282*, 20143127. https://doi.org/10.1098/rspb.2014.3127

Belasen, A. M., Amses, K. R., Clemons, R. A., … James, T. Y. (2022). Habitat fragmentation in the Brazilian Atlantic Forest is associated with erosion of frog immunogenetic diversity and increased fungal infections. *Immunogenetics*, *74*, 431–441. https://doi.org/10.1007/s00251-022-01252-x

Belasen, A. M., Bletz, M. C., da Silva Leite, D., … James, T. Y. (2019). Long-term habitat fragmentation is associated with reduced MHC IIB diversity and increased infections in amphibian hosts. *Frontiers in Ecology and Evolution*, *6*, 236. https://doi.org/10.3389/fevo.2018.00236

Bielby, J., Price, S. J., Monsalve-CarcaÑo, C., & Bosch, J.. (2021). Host contribution to parasite persistence is consistent between parasites and over time, but varies spatially. *Ecological Applications*, *31*, e02256. https://doi.org/10.1002/eap.2256

Bonneaud, C., Mazuc, J., Chastel, O., … Sorci, G. (2004). Terminal investment induced by immune challenge and fitness traits associated with major histocompatibility complex in the house sparrow. *Evolution*, *58*, 2823–2830.

Bosch, J., & Martínez-Solano, I. (2003). Factors influencing occupancy of breeding ponds in a montane amphibian assemblage. *Journal of Herpetology*, *37*, 410–413. https://doi.org/10.1670/0022-1511(2003)037%5b0410:FIOOBP%5d2.0.CO;2

Bosch, J., & Martínez-Solano, I. (2006). Chytrid fungus infection related to unusual mortalities of *Salamandra salamandra* and *Bufo bufo* in the Penalara Natural Park, Spain. *Oryx*, *40*, 84–89. https://doi.org/10.1017/S0030605306000093

Bosch, J., Martı´nez-Solano, I., & Garcı´a-Parı´s, M. (2001). Evidence of a chytrid fungus infection involved in the decline of the common midwife toad (*Alytes obstetricans*) in protected areas of central Spain. *Biological Conservation*, *97*, 331–337. https://doi.org/10.1016/S0006-3207(00)00132-4

Bosch, J., Monsalve-Carcaño, C., Price, S. J., & Bielby, J. (2020). Single infection with *Batrachochytrium dendrobatidis* or *Ranavirus* does not increase probability of co-infection in a montane community of amphibians. *Scientific Reports*, *10*, 21115. https://doi.org/10.1038/s41598-020-78196-3

Bosch, J., Mora-Cabello de Alba, A., Marquínez, S., … Bielby, J. (2021). Long-term monitoring of amphibian populations of a National Park in northern Spain reveals negative persisting effects of *Ranavirus*, but not *Batrachochytrium dendrobatidis*. *Frontiers in Veterinary Science*, *8*, 645491. https://doi.org/10.3389/fvets.2021.645491

Boyle, DG., Boyle, DB., Olsen, V., … Hyatt, AD. (2004). Rapid quantitative detection of chytridiomycosis (Batrachochytrium dendrobatidis) in amphibian samples using real-time Taqman PCR assay. *Diseases of aquatic organisms*, *60*(2), 141–148.

Brown, T., Elewa, A., Iarovenko, S., … Toyoda, A. (2022). Sequencing and chromosome-scale assembly of the giant *Pleurodeles waltl* genome. *bioRxiv*. https://doi.org/10.1101/2022.10.19.512763

Brunner, J. L., Storfer, A., Gray, M. J., & Hoverman, J. T. (2015). *Ranavirus* ecology and evolution: From epidemiology to extinction. In *Ranaviruses*(pp. 71–104). Springer.

Callahan, B. J., McMurdie, P. J., Rosen, M. J., … Holmes, S. P. (2016). DADA2: High-resolution sample inference from Illumina amplicon data. *Nature Methods*, *13*, 581–583. https://doi.org/10.1038/nmeth.3869

Chondrelli, N., Kuehn, E., Meurling, S., … Höglund, J. (2024). *Batrachochytrium dendrobatidis* strain affects transcriptomic response in liver but not skin in latitudinal populations of the common toad (*Bufo bufo*). *Scientific Reports*, *14*, 2495. https://doi.org/10.1038/s41598-024-52975-8

Cortázar-Chinarro, M., Lattenkamp, E. Z., Meyer-Lucht, Y., … Höglund, J. (2017). Drift, selection, or migration? Processes affecting genetic differentiation and variation along a latitudinal gradient in an amphibian. *BMC Evolutionary Biology*, *17*, 1–14.

Cortazar-Chinarro, M., Meurling, S., Schroyens, L., … Höglund, J. (2022). Major histocompatibility complex variation and haplotype associated survival in response to experimental infection of two Bd-GPL strains along a latitudinal gradient. *Frontiers in Ecology and Evolution*, *10*, 915271. https://doi.org/10.3389/fevo.2022.915271

Doherty, P. C., & Zinkernagel, R. M. (1975). Enhanced immunological surveillance in mice heterozygous at the H-2 gene complex. *Nature*, *256*, 50–52. https://doi.org/10.1038/256050a0.

Edholm, E. S., Pasquier, L. D., Wiegertjes, G. F., & Boudinot, P. (2022). Major histocompatibility complex (MHC) in fish. In *Principles of fish immunology*(pp. 355–386). Springer. https://doi.org/10.1007/978-3-030-85420-1

Ejsmond, M. J., & Radwan, J. (2015). Red Queen processes drive positive selection on major histocompatibility complex (MHC) genes. *PLoS Computational Biology*, *11*, e1004627. https://doi.org/10.1371/journal.pcbi.1004627

Eskew, E. A., Shock, B. C., LaDouceur, E. E., … Todd, B. D. (2018). Gene expression differs in susceptible and resistant amphibians exposed to *Batrachochytrium dendrobatidis*. *Royal Society Open Science*, *5*, 170910. https://doi.org/10.1098/rsos.170910

Excoffier, L., & Lischer, H. E. (2010). Arlequin suite ver 3.5: A new series of programs to perform population genetics analyses under Linux and Windows. *Molecular Ecology Resources*, *10*, 564–567. https://doi.org/10.1111/j.1755-0998.2010.02847.x

Fisher, M. C., & Garner, T. W. (2020). Chytrid fungi and global amphibian declines. *Nature Reviews Microbiology*, *18*, 332–343. https://doi.org/10.1038/s41579-020-0335-x

Flechoso, M. F., Alarcos, G., & Jara, R. (2019). Primer caso documentado de ranavirosis en Castilla y León en una población de gallipato, *Pleurodeles waltl* Michahelles, 1830. *Boletín De La Asociación Herpetológica Española*, *30*, 48–52.

Fu, M., & Waldman, B. (2017). Major histocompatibility complex variation and the evolution of resistance to amphibian chytridiomycosis. *Immunogenetics*, *69*, 529–536. https://doi.org/10.1007/s00251-017-1008-4

Fu, M., Eimes, J. A., & Waldman, B. (2023). Divergent allele advantage in the MHC and amphibian emerging infectious disease. *Infection, Genetics and Evolution*, *111*, 105429. https://doi.org/10.1016/j.meegid.2023.105429

Garamszegi, L. Z., Zagalska-Neubauer, M., Canal, D., … Török, J. (2015). Malaria parasites, immune challenge, MHC variability, and predator avoidance in a passerine bird. *Behavioral Ecology*, *26*, 1292–1302. https://doi.org/10.1093/beheco/arv077

Grieves, L., Gloor, G., Bernards, M., & MacDougall-Shackleton, E. (2019). Songbirds show odour-based discrimination of similarity and diversity at the major histocompatibility complex. *Animal Behaviour*, *158*, 131–138. https://doi.org/10.1016/j.anbehav.2019.10.005

Hablützel, P. I., Vanhove, M., Grégoir, A., … Raeymaekers, J. (2014). Intermediate number of major histocompatibility complex class IIB length variants relates to enlarged perivisceral fat deposits in the blunt-head cichlid *Tropheus moorii*. *Journal of Evolutionary Biology*, *27*, 2177–2190. https://doi.org/10.1111/jeb.12467

Harrison, X. A. (2014). Using observation-level random effects to model overdispersion in count data in ecology and evolution. *PeerJ*, *2*, e616. https://doi.org/10.7717/peerj.616

Hartig, F., & Hartig, M. F. (2017). *Package 'DHARMa'*. R Package.

Heijmans, C. M., de Groot, N. G., & Bontrop, R. E. (2020). Comparative genetics of the major histocompatibility complex in humans and nonhuman primates. *International Journal of Immunogenetics*, *47*, 243–260. https://doi.org/10.1111/iji.12490.

Herczeg, D., Ujszegi, J., Kásler, A., … Hettyey, A. (2021). Host–multiparasite interactions in amphibians: A review. *Parasites & Vectors*, *14*, 1–20. https://doi.org/10.1186/s13071-021-04796-1

Hoarau, A. O., Mavingui, P., & Lebarbenchon, C. (2020). Coinfections in wildlife: Focus on a neglected aspect of infectious disease epidemi-

ology. *PLoS Pathogens*, *16*, e1008790. https://doi.org/10.1371/journal.ppat.1008790
Hoverman, J. T., Mihaljevic, J. R., Richgels, K. L., … Johnson, P. T. (2012). Widespread co-occurrence of virulent pathogens within California amphibian communities. *EcoHealth*, *9*, 288–292. https://doi.org/10.1007/s10393-012-0778-2
Huson, D. H., & Bryant, D. (2006). Application of phylogenetic networks in evolutionary studies. *Molecular Biology and Evolution*, *23*, 254–267. https://doi.org/10.1093/molbev/msj030
Ivy-Israel, N., Moore, C. E., Schwartz, T. S., & Ditchkoff, S. S. (2020). Characterization of two MHC II genes (DOB, DRB) in white-tailed deer (*Odocoileus virginianus*). *BMC Genetics*, *21*, 1–17. https://doi.org/10.1186/s12863-020-00889-5
Jan Ejsmond, M., Radwan, J., & Wilson, A. B. (2014). Sexual selection and the evolutionary dynamics of the major histocompatibility complex. *Proceedings of the Royal Society B: Biological Sciences*, *281*, 20141662. https://doi.org/10.1098/rspb.2014.1662
Jones, E. Y., Fugger, L., Strominger, J. L., & Siebold, C. (2006). MHC class II proteins and disease: A structural perspective. *Nature Reviews Immunology*, *6*, 271–282. https://doi.org/10.1038/nri1805
Kalbe, M., Eizaguirre, C., Dankert, I., … Milinski, M. (2009). Lifetime reproductive success is maximized with optimal major histocompatibility complex diversity. *Proceedings of the Royal Society B: Biological Sciences*, *276*, 925–934. https://doi.org/10.1098/rspb.2008.1466
Kaufman, J. F., Flajnik, M. F., Du Pasquier, L., & Riegert, P. (1985). Xenopus MHC class II molecules. I. Identification and structural characterization. *The Journal of Immunology*, *134*, 3248–3257. https://doi.org/10.4049/jimmunol.134.5.3248
Kiemnec-Tyburczy, K., Richmond, J., Savage, A., … Zamudio, K. (2012). Genetic diversity of MHC class I loci in six non-model frogs is shaped by positive selection and gene duplication. *Heredity*, *109*, 146–155. https://doi.org/10.1038/hdy.2012.22
Klein, J. (1975). *Biology of the mouse histocompatibility-2 complex: principles of immunogenetics applied to a single system*, Vol. *12*, (p. 620). Springer-Verlag, New York.
Klein, J. (1979). The major histocompatibility complex of the mouse. *Science*, *203*, 516–521. https://doi.org/10.1126/science.104386
Kloch, A., Babik, W., Bajer, A., … Radwan, J. (2010). Effects of an MHC-DRB genotype and allele number on the load of gut parasites in the bank vole *Myodes glareolus*. *Molecular Ecology*, *19*, 255–265. https://doi.org/10.1111/j.1365-294X.2009.04476.x
Kumar, S., Stecher, G., Li, M., & Tamura, K. (2018). MEGA X: Molecular evolutionary genetics analysis across computing platforms. *Molecular Biology and Evolution*, *35*, 1547. https://doi.org/10.1093/molbev/msy096
Lenth, R., Singmann, H., Love, J., … Herve, M. (2019). *Package 'emmeans'*.
Leung, W.T.M., Thomas-Walters, L., Garner, T.W.J., … Price, S.J. (2017). A quantitative-PCR based method to estimate ranavirus viral load following normalisation by reference to an ultraconserved vertebrate target. *Journal of Virological Methods*, *249*, 147–155.
Lighten, J., Van Oosterhout, C., Paterson, I. G., … Bentzen, P. (2014). Ultra-deep Illumina sequencing accurately identifies MHC class II b alleles and provides evidence for copy number variation in the guppy (*Poecilia reticulata*). *Molecular Ecology Resources*, *14*, 753–767. https://doi.org/10.1111/1755-0998.12225
Madsen, T., & Ujvari, B. (2006). MHC class I variation associates with parasite resistance and longevity in tropical pythons. *Journal of Evolutionary Biology*, *19*, 1973–1978. https://doi.org/10.1111/j.1420-9101.2006.01158.x
Magnusson, A., Skaug, H., Nielsen, A., … Brooks, M. M. (2017). *Package 'glmmtmb'. R Package Version 0.2.0*.
Magoč, T., & Salzberg, S. L. (2011). FLASH: Fast length adjustment of short reads to improve genome assemblies. *Bioinformatics*, *27*, 2957–2963.
Martel, A., Blooi, M., Adriaensen, C., … Goka, K. (2014). Recent introduction of a chytrid fungus endangers Western Palearctic salamanders. *Science*, *346*, 630–631. https://doi.org/10.1126/science.1258268
May, S., Zeisset, I., & Beebee, T. J. (2011). Larval fitness and immunogenetic diversity in chytrid-infected and uninfected natterjack toad (*Bufo calamita*) populations. *Conservation Genetics*, *12*, 805–811. https://doi.org/10.1007/s10592-011-0187-z
McDonald, C. A., Becker, C. G., Lambertini, C., … Zamudio, K. R. (2023). Host immune responses to enzootic and invasive pathogen lineages vary in magnitude, timing, and efficacy. *Molecular Ecology*, *32*, 2252–2270. https://doi.org/10.1111/mec.16890
Meyer-Lucht, Y., & Sommer, S. (2009). Number of MHC alleles is related to parasite loads in natural populations of yellow necked mice, *Apodemus flavicollis*. *Evolutionary Ecology Research*, *11*, 1085–1097.
Migalska, M., Przesmycka, K., Alsarraf, M., … Radwan, J. (2022). Long term patterns of association between MHC and helminth burdens in the bank vole support Red Queen dynamics. *Molecular Ecology*, *31*, 3400–3415. https://doi.org/10.1111/mec.16486
Milinski, M. (2006). The major histocompatibility complex, sexual selection, and mate choice. *Annual Review of Ecology, Evolution, and Systematics*, *37*, 159–186. https://doi.org/10.1146/annurev.ecolsys.37.091305.110242
Miller, D., Gray, M., & Storfer, A. (2011). Ecopathology of ranaviruses infecting amphibians. *Viruses*, *3*, 2351–2373. https://doi.org/10.3390/v3112351
Minias, P., Palomar, G., Dudek, K., & Babik, W. (2022). Salamanders reveal novel trajectories of amphibian MHC evolution. *Evolution*, *76*, 2436–2449. https://doi.org/10.1111/evo.14601
Mulder, K. P., Cortazar-Chinarro, M., Harris, D. J., … Savage, A. E. (2017). Evolutionary dynamics of an expressed MHC class IIβ locus in the Ranidae (Anura) uncovered by genome walking and high-throughput amplicon sequencing. *Developmental & Comparative Immunology*, *76*, 177–188. https://doi.org/10.1016/j.dci.2017.05.022
Nowak, M. A., Tarczy-Hornoch, K., & Austyn, J. M. (1992). The optimal number of major histocompatibility complex molecules in an individual. *Proceedings of the National Academy of Sciences*, *89*, 10896–10899. https://doi.org/10.1073/pnas.89.22.10896
O'Reilly, R. L., Paterson, J. S., Mitchell, J. G., & Gardner, M. G. (2023). Viral abundance and sub-population variation in *Tiliqua rugosa* over an ecological gradient using flow cytometry. In *Exploration of host-pathogen interactions in the Australian skink Tiliqua rugosa*.
Olori, J. C., Netzband, R., McKean, N., … Windstam, S. T. (2018). Multi-year dynamics of *Ranavirus*, chytridiomycosis, and co-infections in a temperate host assemblage of amphibians. *Diseases of Aquatic Organisms*, *130*, 187–197. https://doi.org/10.3354/dao03260
Osborne, M. J., Pilger, T. J., Lusk, J. D., & Turner, T. F. (2017). Spatiotemporal variation in parasite communities maintains diversity at the major histocompatibility complex class IIβ in the endangered Rio Grande silvery minnow. *Molecular Ecology*, *26*, 471–489. https://doi.org/10.1111/mec.13936
Palomar, G., Bosch, J., & Cano, J. M. (2016). Heritability of *Batrachochytrium dendrobatidis* burden and its genetic correlation with development time in a population of Common toad (*Bufo spinosus*). *Evolution*, *70*, 2346–2356. https://doi.org/10.1111/evo.13029
Palomar, G., Dudek, K., Migalska, M., … Shaffer, H. B. (2021). Co-evolution between MHC class I and antigen-processing genes in salamanders. *Molecular Biology and Evolution*, *38*, 5092–5106. https://doi.org/10.1093/molbev/msab237
Papadopoulos, G., Bondinas, G., & Moustakas, A. (2008). The murine pro-insulin II molecule contains strong-binding motifs for several H2-A and H2-E alleles that protect NOD mice from diabetes. In *Diabetologia*(Vol. *51*.pp. S227–S227). Springer.
Penn, D. J., & Potts, W. K. (1999). The evolution of mating preferences and major histocompatibility complex genes. *The American Naturalist*, *153*(2), 145–164.
Penn, D. J., Damjanovich, K., & Potts, W. K. (2002). MHC heterozygosity confers a selective advantage against multiple-strain infec-

tions. *Proceedings of the National Academy of Sciences*, *99*, 11260–11264. https://doi.org/10.1073/pnas.162006499

Phillips, K. P., Cable, J., Mohammed, R. S., … Radwan, J. (2018). Immunogenetic novelty confers a selective advantage in host–pathogen coevolution. *Proceedings of the National Academy of Sciences*, *115*, 1552–1557. https://doi.org/10.1073/pnas.1708597115

Price, S. J., Garner, T. W., Nichols, R. A., … Bosch, J. (2014). Collapse of amphibian communities due to an introduced *Ranavirus*. *Current Biology*, *24*, 2586–2591. https://doi.org/10.1016/j.cub.2014.09.028

R Core Team. (2021). R: A language and environment for statistical computing.. R Foundation for Statistical Computing, Vienna, Austria. https://www.R-project.org/

Råberg, L., Clough, D., Hagström, Å., … Westerdahl, H. (2022). MHC class II genotype-by-pathogen genotype interaction for infection prevalence in a natural rodent-Borrelia system. *Evolution*, *76*, 2067–2075. https://doi.org/10.1111/evo.14590

Radwan, J., Babik, W., Kaufman, J., … Winternitz, J. (2020). Advances in the evolutionary understanding of MHC polymorphism. *Trends in Genetics*, *36*, 298–311. https://doi.org/10.1016/j.tig.2020.01.008

Radwan, J., Zagalska-Neubauer, M., Cichoń, M., & Babik, W. (2012). MHC diversity, malaria and lifetime reproductive success in collared flycatchers. *Molecular Ecology*, *21*, 2469–2479. https://doi.org/10.1111/j.1365-294X.2012.05547.x

Reed, K. M., & Settlage, R. E. (2021). Major histocompatibility complex genes and locus organization in the Komodo dragon (*Varanus komodoensis*). *Immunogenetics*, *73*, 405–417. https://doi.org/10.1007/s00251-021-01217-6

Robinson, D. (2014). broom: An R package for converting statistical analysis objects into tidy data frames. *arXiv* preprint arXiv:1412.3565.

Savage, A. E., & Zamudio, K. R. (2011). MHC genotypes associate with resistance to a frog-killing fungus. *Proceedings of the National Academy of Sciences*, *108*, 16705–16710. https://doi.org/10.1073/pnas.1106893108

Savage, A. E., & Zamudio, K. R. (2016). Adaptive tolerance to a pathogenic fungus drives major histocompatibility complex evolution in natural amphibian populations. *Proceedings of the Royal Society B: Biological Sciences*, *283*, 20153115. https://doi.org/10.1098/rspb.2015.3115

Savage, A. E., Gratwicke, B., Hope, K., … Fleischer, R. C. (2020). Sustained immune activation is associated with susceptibility to the amphibian chytrid fungus. *Molecular Ecology*, *29*, 2889–2903. https://doi.org/10.1111/mec.15533

Savage, A. E., Muletz-Wolz, C. R., Campbell Grant, E. H., … Mulder, K. P. (2019). Functional variation at an expressed MHC class IIβ locus associates with *Ranavirus* infection intensity in larval anuran populations. *Immunogenetics*, *71*, 335–346. https://doi.org/10.1007/s00251-019-01104-1

Scheele, B. C., Pasmans, F., Skerratt, L. F., … Catenazzi, A. (2019). Amphibian fungal panzootic causes catastrophic and ongoing loss of biodiversity. *Science*, *363*, 1459–1463. https://doi.org/10.1126/science.aav0379

Sebastian, A., Herdegen, M., Migalska, M., & Radwan, J. (2016). amplisas: a web server for multilocus genotyping using next-generation amplicon sequencing data. *Molecular Ecology Resources*, *16*(2), 498–510.

Sepil, I., Lachish, S., & Sheldon, B. C. (2013). MHC-linked survival and lifetime reproductive success in a wild population of great tits. *Molecular Ecology*, *22*, 384–396. https://doi.org/10.1111/mec.12123

Skerratt, L. F., Berger, L., Speare, R., … Kenyon, N. (2007). Spread of chytridiomycosis has caused the rapid global decline and extinction of frogs. *EcoHealth*, *4*, 125–134. https://doi.org/10.1007/s10393-007-0093-5

Slade, J. W., Sarquis-Adamson, Y., Gloor, G. B., … MacDougall-Shackleton, E. A. (2017). Population differences at MHC do not explain enhanced resistance of song sparrows to local parasites. *Journal of Heredity*, *108*, 127–134

Solt, F., & Hu, Y. (2015). *dotwhisker: Dot-and-whisker plots of regression results*. Comprehensive R Archive Network (CRAN).

Sommer, S. (2005). The importance of immune gene variability (MHC) in evolutionary ecology and conservation. *Frontiers in Zoology*, *2*, 1–18. https://doi.org/10.1186/1742-9994-2-16

Spurgin, L. G., & Richardson, D. S. (2010). How pathogens drive genetic diversity: MHC, mechanisms and misunderstandings. *Proceedings of the Royal Society B: Biological Sciences*, *277*, 979–988. https://doi.org/10.1098/rspb.2009.2084

Stervander, M., Dierickx, E. G., Thorley, J., … Westerdahl, H. (2020). High MHC gene copy number maintains diversity despite homozygosity in a critically endangered single-island endemic bird, but no evidence of MHC-based mate choice. *Molecular Ecology*, *29*, 3578–3592. https://doi.org/10.1111/mec.15471

Stutz, W. E., Blaustein, A. R., Briggs, C. J., … Johnson, P. T. (2018). Using multi-response models to investigate pathogen coinfections across scales: Insights from emerging diseases of amphibians. *Methods in Ecology and Evolution*, *9*, 1109–1120. https://doi.org/10.1111/2041-210X.12938

Talarico, L., Babik, W., Marta, S., … Mattoccia, M. (2019). MHC structuring and divergent allele advantage in a urodele amphibian: A hierarchical multi-scale approach. *Heredity*, *123*, 593–607. https://doi.org/10.1038/s41437-019-0221-3

Thoss, M., Ilmonen, P., Musolf, K., & Penn, D. (2011). Major histocompatibility complex heterozygosity enhances reproductive success. *Molecular Ecology*, *20*, 1546–1557. https://doi.org/10.1111/j.1365-294X.2011.05009.x

Thumsová, B., Alarcos, G., Ayres, C., … Bosch, J. (2024). Relationship between two pathogens in an amphibian community that experienced mass mortalities. *Conservation Biology*, *38*, e14196. https://doi.org/10.1111/cobi.14196

Thumsová, B., Bosch, J., & Rosa, G. M. (2023). Amphibian crisis and the impact of emerging pathogens. In G. Moreno-Rueda & M. Comas (Eds.), *Evolutionary ecology of amphibians*(pp. 54–102). CRC Press.https://doi.org/10.1201/9781003093312

Thumsová, B., Price, S. J., González-Cascón, V., … Bosch, J. (2022). Climate warming triggers the emergence of native viruses in Iberian amphibians. *Iscience*, *25*, 105541. https://doi.org/10.1016/j.isci.2022.105541

Trujillo, A. L., Hoffman, E. A., Becker, C. G., & Savage, A. E. (2021). Spatiotemporal adaptive evolution of an MHC immune gene in a frog-fungus disease system. *Heredity*, *126*, 640–655. https://doi.org/10.1038/s41437-020-00402-9

van Oosterhout, C. (2009). A new theory of MHC evolution: Beyond selection on the immune genes. *Proceedings of the Royal Society B: Biological Sciences*, *276*, 657–665. https://doi.org/10.1098/rspb.2008.1299

Warne, R. W., LaBumbard, B., LaGrange, S., … Catenazzi, A. (2016). Co-infection by chytrid fungus and ranaviruses in wild and harvested frogs in the tropical Andes. *PLoS ONE*, *11*, e0145864. https://doi.org/10.1371/journal.pone.0145864

Wegner, K. M., Kalbe, M., Kurtz, J., … Milinski, M. (2003). Parasite selection for immunogenetic optimality. *Science*, *301*, 1343–1343. https://doi.org/10.1126/science.1088293

Wegner, K. M., Kalbe, M., Milinski, M., & Reusch, T. B. (2008). Mortality selection during the 2003 European heat wave in three-spined sticklebacks: Effects of parasites and MHC genotype. *BMC Evolutionary Biology*, *8*, 1–12. https://doi.org/10.1186/1471-2148-8-124

Westerdahl, H. (2007). Passerine MHC: Genetic variation and disease resistance in the wild. *Journal of Ornithology*, *148*, 469–477. https://doi.org/10.1007/s10336-007-0230-5

Whitfield, S. M., Geerdes, E., Chacon, I., … Kerby, J. L. (2013). Infection and co-infection by the amphibian chytrid fungus and *Ranavirus* in wild Costa Rican frogs. *Diseases of Aquatic Organisms*, *104*, 173–178. https://doi.org/10.3354/dao02598

Whittingham, L. A., Freeman-Gallant, C. R., Taff, C. C., & Dunn, P. O. (2015). Different ornaments signal male health and MHC variation

in two populations of a warbler. *Molecular Ecology*, *24*, 1584–1595. https://doi.org/10.1111/mec.13130

Wickham, H. (2011). ggplot2. *WIREs Computational Statistics*, *3*, 180–185. https://doi.org/10.1002/wics.147

Winternitz, J., Minchey, S., Garamszegi, L. Z., … Altizer, S. (2013). Sexual selection explains more functional variation in the mammalian major histocompatibility complex than parasitism. *Proceedings of the Royal Society B: Biological Sciences*, *280*, 20131605. https://doi.org/10.1098/rspb.2013.1605

Woelfing, B., Traulsen, A., Milinski, M., & Boehm, T. (2009). Does intra-individual major histocompatibility complex diversity keep a golden mean? *Philosophical Transactions of the Royal Society B: Biological Sciences*, *364*, 117–128. https://doi.org/10.1098/rstb.2008.0174

Appendix

Appendix 1. PCR information

We amplified major histocompatibility complex (MHC) class II exon 2 fragments of varying lengths across the three species: 252 bp in *P. perezi*, 239 bp in *I. Alpestris*, and 355bp in *P. waltl*. As the primers used had not been used previously for MHC class II exon 2 amplification in *P. waltl* and *P. perezi*, PCR products were visualized and isolated from 1.5% agarose gels. The resulting product was sequenced for DNA-sequence and fragment length verification. All PCR products were standard Sanger-sequenced at Macrogen Europe (Netherlands). For Illumina MiSeq sequencing preparation, both forward and reverse primers were modified with an individual 8-bp barcode and a sequence of three N to facilitate cluster identification. Each sample was given a unique individual combination of a forward and a reverse barcode for identification. PCR reactions were conducted in 20 μl reactions containing 1 μl of genomic DNA, 2 μl of 10X Dream taq buffer (Thermo scientific AB), 0.4 μl of 2 mM of each dNTP, 0.5 μl of each 10 μM primer (TrMHCII1F/TrMHCII5R and ForN/RevM, respectively), 1.5 μl of bovine serum albumin (BSA; 5 mg/ml), and 0.25 μl of Dream taq DNA polymerase (5 U/μl, Thermo Scientific Lab) in deionized water. Thermocycling was performed on an ABI 2720 thermocycler (Applied Biosystems) with the following protocol: An initial denaturation step of 3 min at 95 °C, followed by 30 cycles of 30 s at 95 °C, annealing for 30 s at 70 °C (*I. alpestris* and *P. waltl*) and 62°C (*P. perezi*), and an extension step at 72 °C for 1 min.

To prevent contamination, all amplifications were carried out using filter tips in separate pre- and post-PCR rooms, with negative controls included following Cortazar-Chinarro et al. (2017). PCR products were run and visualized on a 1.5% agarose gel using gelgreen (BIOTIUM). To reduce the number of samples for subsequent purification, three to nine PCR products with similar concentrations were pooled based on gel image estimations. These pools were run on 1.5% agarose gel, and the target band excised from the gel and extracted using the MinElute Gel Extraction Kit (Qiagen Sollentuna, Sweden). The sample pool concentrations were measured with Quant-iT PicoGreen dsDNA assay kit (Invitrogen Life Technologies, Stockholm, Sweden) on a fluorescence microplate reader (Ultra 384; Tecan Group Ltd., Männedorf, Switzerland). Final amplicon pooling combined equimolecular amounts of each sample. Six amplicon pools were generated per run, with libraries prepared using the Illumina Truseq DNA PCR-Free Sample preparation kit (Illumina Inc., San Diego, CA). Six pools were combined into a Miseq run (PE250). Sequencing of two Miseq runs was carried out at the National Genomic Infrastructure (NGI), the SNP&SEQ Technology Platform hosted at SciLifeLab in Uppsala (Sweden).

Cortázar-Chinarro, M., Lattenkamp, E.Z., Meyer-Lucht, Y., Luquet, E., Laurila, A., & Höglund, J. (2017). Drift, selection, or migration? Processes affecting genetic differentiation and variation along a latitudinal gradient in an amphibian. *BMC Evolutionary Biology*, *17*, 1–14.

Appendix 2. Number of MHC allele II exon 2 copies in studied species

The MHC has been characterized in a variety of taxa, including fish (Edholm et al., 2022), primates (Heijmans et al., 2020), ungulates (Ivy-Israel et al., 2020), reptiles (Reed & Settlage, 2021), and amphibian species (Cortázar-Chinarro et al., 2017; Kiemnec-Tyburczy et al., 2012; Palomar et al., 2021; Talarico et al., 2019). A previous characterization of MHC II in *I. alpestris* from Southern Poland revealed high genetic variation, with a maximum of nine alleles per individual, suggesting the presence of at least five loci in this Eastern European population (Babik et al., 2008). In contrast, our study found a maximum of six alleles per individual, indicating the existence of at least three loci in the same species. This difference could arise from either varying number of loci or from allele sharing between MHC copies within the Spanish population. However, we cannot exclude the possibility of copy number differences between populations or from variable amplification success of different alleles. Additional immunogenetic studies are needed to characterize MHC genetic diversity in *I. alpestris* across its geographical distribution.

Our study presents the first characterization of MHC II in *P. perezi* and *P. waltl*. While *P. perezi* exhibited high MHC II genetic diversity, *P. waltl* showed relatively low variation. In *P. waltl*, we identified only four different MHC alleles (Pleu_wa*01, 02, 05, 07), with two of them (Pleu_wa*05, 07) occurring at very low frequencies. The recent publication of the *P. waltl* genome (Brown et al., 2022) confirmed the presence of at least one MHC II gene in this species, suggesting that *P. waltl* may possess lower genetic diversity in this region compared to other species with multiple MHC II genes. Our analysis of 57 individuals revealed only four alleles for this gene, which is typically associated with low diversity levels. This reduced variation could result from mass mortalities attributed to *Bd* or *Rv*, which might have selectively favoured resistant alleles, or alternatively, from a bottleneck or genetic drift. Further research comparing populations affected by emerging diseases with unaffected populations could provide valuable insights into this pattern.

Received August 22, 2024; revised August 19, 2025; accepted September 4, 2025